ACTA MECHANICA SINICA, Vol.7, No.4, November 1991
Science Press, Beijing, China
Allerton Press, INC., New York, U.S.A.
ISSN 0567 – 7718

# THE APPLICATION OF MOIRE INTERFEROMETRY IN THE MEASUREMENT OF DISPLACEMENT FIELD AND STRAIN FIELD AT NOTCH-TIP AND CRACK-TIP*

Han Jinhu (韩金虎) Mao Tianxiang (毛天祥)
(*Institute of Mechanics, Chinese Academy of Sciences, Beijing* 100080, *China*)

**ABSTRACT**: This paper presents the application of Moire interferometry in measuring the displacement and strain field at notch-tip and crack-tip before and after crack propagation. The experiment is carried out using a three point bending beam with a notch. The $N_x$ and $N_y$ fringe patterns representing displacement field, and the $\Delta N_x/\Delta x$ and $\Delta N_y/\Delta y$ fringe patterns representing the strain field are obtained. The sensitivity of the measured displacement is 0.417 $\mu$m per fringe order. The displacement and strain distribution along the section $x=0$ have been worked out according to $N_x$ and $N_y$ fringe patterns.

**KEY WORDS**: moire interferometry, displacement field, strain field, necking zone

## I. INTRODUCTION

The experimental determination of displacement field and strain field at notch-tip or crack-tip is especially important. It provides experiment data to verify computational methods and their results, and it also offers helpful data for engineering design and verification. Among many experimental methods available for measuring displacement field and strain field (grids, geometriec moire, speckle interferometry, moire interferometry, moire interferometry of sticking film, etc.) moire interferometry is the best. Moire interferometry is a whole-field quantitative optical method for determining in-plane displacement field of an opaque bodies. The strain field is obtained by mechanical differentiation. This method of experimental mechanics enjoys high sensitivity, excellent fringe contrast, high spatial resolution, and extensive range. Its pattern location is coincident with specimen and it is real-time. Moire interferometry provides a perfect method for determination of displacement field and strain field at notch-tip or crack-tip.

## II. EXPERIMENTAL ARRANGEMENT FOR MOIRE INTERFEROMETRY

A schematic diagram of experimental arrangement for moire interferometry is shown in Fig.1. A high-frequency cross-line diffraction grating is replicated on the surface of specimen with frequency $f/2=1200$ line/mm. The replication process of the grating is detailed in Ref.[1].

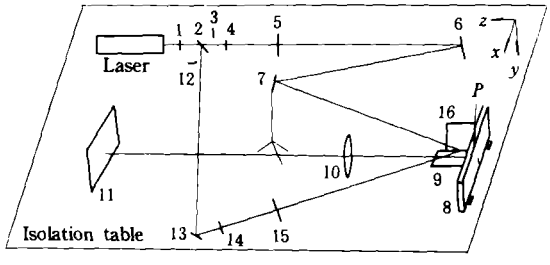


Fig.1

1 Electric shutter, 2 Beam splitter, 3 Shutter, 4 Beam expander, 5 Collimating lens ($\varphi$ 120), 6 Mirror ($\varphi$ 100), 7 Mirror (70 × 100), 8 Specimen, 9 Mirror (70 × 100), 10 Camera lens, 11 groundglass or filmholder with micrometer for x and y direction, 12 Shutter, 13 Mirror, 14 Beam expander, 15 Collimating, 16 Mirror

Received 29 March 1991, revised 1 May 1991
* The project supported by Chinese Academy of Sciences and National Natural Science Foundation of China

The specimen grating is firmly attached to the specimen surface. When the loads are applied to the specimen, the specimen grating starts to move and deform together with the specimen surface. Before adjusting arrangement the camera lens 10 is removed temporarily. The laser beam passes through the electric shutter 1. If the shutter 12 is shut and the shutter 3 is opened, the laser beam passes through the expander 4. The collimated beam will be formed by using a collimaling lens 5. The collimated beam is reflected by the mirror 6 and is projected to the mirror 7, which is located on the tripod of camera and may be adjusted by rotating around $x$-axis and $y$-axis. The half of collimated beam strikes directly at the specimen. The other half strikes indirectly at the specimen in a symmetrical direction after reflection from the mirror 9 which can be adjusted by rotating around $x$-axis and $z$-axis.

The images of $+1$ and $-1$ diffraction orders of the specimen grating with lines perpendicular to $y$ direction will appear in the groundglass 11. With noload on the specimen the images should be merged into one by adjusting the mirror 7 and the mirror 9. This adjusting is for measuring the deformation in $y$ direction. If the shutter 3 is shut and shutter 12 is opened, the measurement of deformation in $x$ direction is performed in the same way as that in $y$ direction. The fringe patterns of the image on the groundglass are formed by interference between beams with $+1$ and $-1$ diffraction orders. This arrangement is recognized as a geometric moire with fringe-multiplication factor of 2. Because the frequency of specimen grating is $f/2$, the frequency of grating to form fringe patterns should be $f/2\times 2=f$ on moire interferometry. An interpretation of moire interferometry from wave front interference theory was provided in [2]. The magnified image appears on the groundglass when the camera lens 10 is located in an appropriate position. The distance between camera lens and groundglass is adjusted for an image of the specimen surface to focus exactly on the groundglass. While the fringes of two-beam interference are nonlocalized and it can result in a good contrast at every position. So the adjustment should provide a focused image of the boundaries of the specimen. If the groundglass is replaced by the filmholder, after turning off the light and fitting the film in the filmholder, the fringe pattens can be photographed with the electric shutter.

The fringe patterns of moire interferometry depict the in-plane displacement at every point on the specimen surface as a contour maps of displacements governed by the quantitative relationship as follows

$$u=\frac{1}{f}\cdot N_x \tag{1}$$

$$v=\frac{1}{f}\cdot N_y \tag{2}$$

where $u$ and $v$ are displacement components in $x$ and $y$ directions, respectively; $N_x$, $N_y$ are fringe orders, $f$ is the frequency. The strains can be calculated from displacement fields by the following relations

$$\varepsilon_x=\frac{\partial u}{\partial x}=\frac{1}{f}\cdot\frac{\partial N_x}{\partial x}$$

$$\varepsilon_y=\frac{\partial v}{\partial y}=\frac{1}{f}\cdot\frac{\partial N_y}{\partial y}$$

If the fringes are dense, the partial derivatives can be approximated in their finite increment form:

$$\varepsilon_x=\frac{1}{f}\cdot\frac{\Delta N_x}{\Delta x} \tag{3}$$

$$\varepsilon_x=\frac{1}{f}\cdot\frac{\Delta N_x}{\Delta x} \tag{4}$$

When $\Delta x=\Delta y=\Delta$, a constant can be identified, namely,

$$\frac{1}{f\Delta}=\text{sensitivity factor} \tag{5}$$

which defines the sensitivity in strain per fringe order for the strain field. Techniques of mechanical differentiation can be used to produce whole-fleld contour maps of difference of displacements. As practical implementation, the double exposure method was used in conjunction with a movable filmholder, The specimen is loaded and the exposure of the $u$ field is made. Then the filmholder is shifted by an increment $\Delta x$ to make a second exposure on the same film. The above process was repeated for the $v$ displacement field. The contour maps of $\Delta N_x/\Delta x$ and $\Delta N_y/\Delta y$ for the strain distribution are obtained. They can be used to obtain the strain field approximately. There are also fringes of displacement field on the contour maps of $\Delta N_x/\Delta x$ and $\Delta N_y/\Delta y$. Fringes of displacement field on the contour maps of $\Delta N_x/\Delta x$ and $\Delta N_y/\Delta y$ could be removed[1] to get a clear background. The strain distribution at a section of specimen can also be obtained from the displacement field directly by Eq. (3) or (4). For example, since $\Delta N_x=1$ between adjacent fringes, if the measured distance between adjacent fringes $\Delta x=\delta$, the frenqency is $f$ and the pitch $p=1/f$, then Eq.(3) becomes

$$\varepsilon_x=\frac{p}{\delta} \tag{6}$$

The strain $\varepsilon_y$ can be obtained in the same way.

## III. THE MEASUREMENT OF DISPLACEMENT FIELD AND STRAIN FIELD ON THE THREE POINT BENDING BEAM WITH NOTCH

A specimen is made of aluminum-alloy LY-12 as shown in Fig.2. The diffraction grating with high frequency cross lines was previously replicated on the specimen surface, the frequency of specimen grating is $f/2=1200$ lines/mm in both $x$ and $y$ directions. The notch on the specimen was produced by electric spark of molybdenum wire. The radius of curvature at the notch-tip is 0.06 mm.

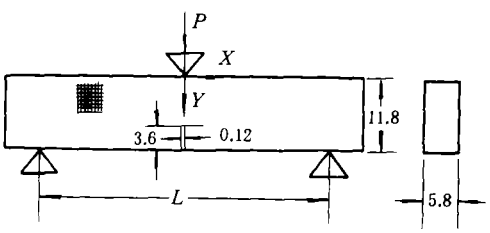


Fig.2 Specimen and loading
first experiment: $L=44$ mm, second experiment: $L=48$ mm

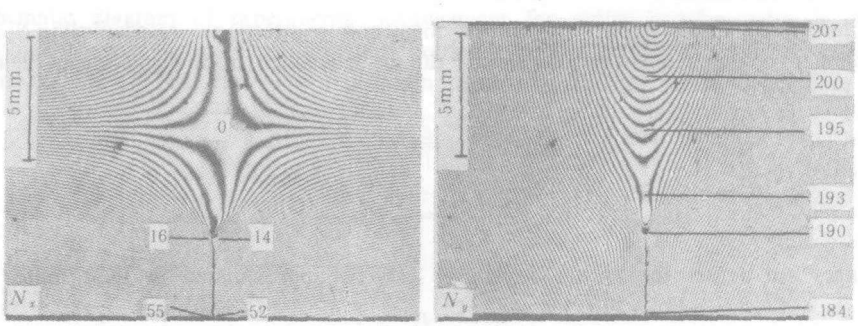


Fig.3 $N_x$ and $N_y$ fringe patterns ($u$ and $v$ field) for load $P=1775$ N, fringe interval 0.417 $\mu$m. The numbers are fringe orders

In the present work two experiments were performed on the same specimen. The number of fringes without loading can be made as small as desired by adjusting the apparatus. The field of view of the image is so small that magnification must be used to obtain the fringe pattern. Therefore the effect of initial fringes could be neglected in the present work.

The specimen was loaded in three steps, with loads 1775N, 2485N and 3195N, respectively,

in the first experiment. When the specimen was loaded to 3195N (maximum loading capability of the loading frame) the necking zone at the notch-tip appeared, but the crack was not generated at the notch-tip. Representative moire interferometry fringe patterns of $N_x$ and $N_y$ are shown in Fig .3 for load $P=1775$N. They signify the contour maps of displacement distribution. Fig .4 is the $N_x$ and $N_y$ fringe patterns of local zone at the notch-tip for load $P=3195$N. The fringes can be observed also at the necking zone. Fig .5 gives $\Delta N_x/\Delta x$ and $\Delta N_y/\Delta y$ fringe patterns of local zone at the notch-tip .

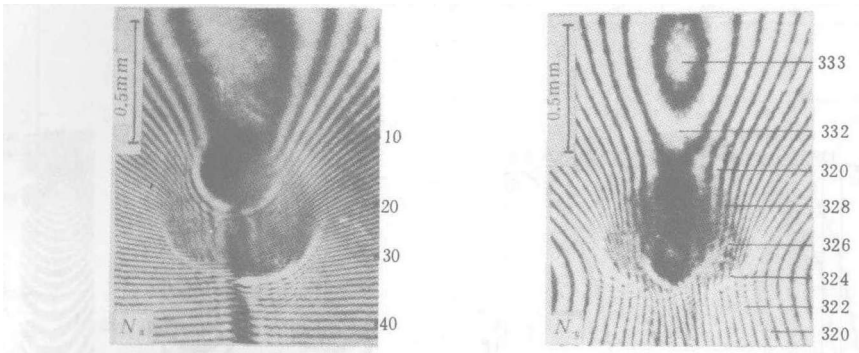


Fig .4 $N_X$ and $N_y$ fringe patterns ($u$ and $v$ field) for load $P=3195$N, fringe interval 0.417$\mu$m. The numbers are fringe orders

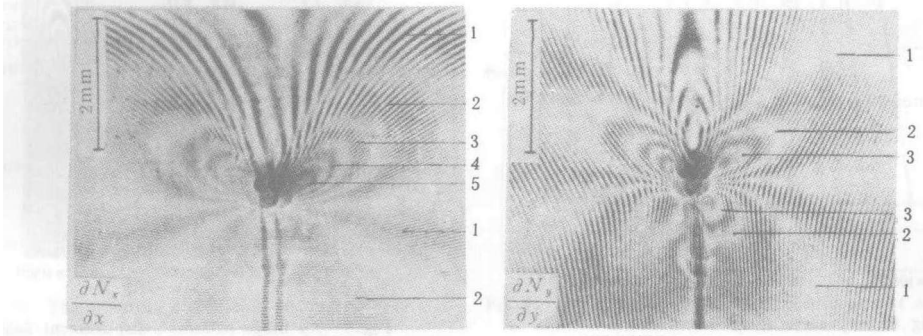


Fig .5 $\Delta N_x/\Delta x$ and $\Delta N_y/\Delta y$ fringe patterns ($\varepsilon_x$ and $\varepsilon_y$ field) for $P=3195$N, $\Delta x=\Delta y=0.24$mm, $1/f\Delta=0.00174$ (sensitivity factor). The numbers are fringe orders

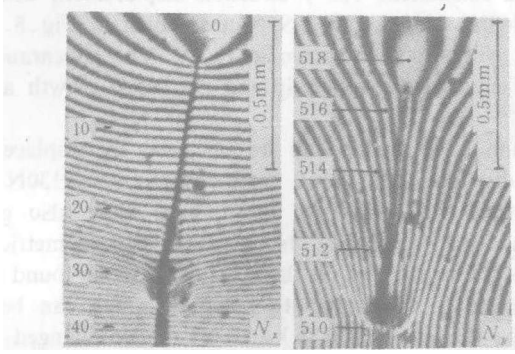


Fig .6 $N_x$ and $N_y$ fringe patterns ($u$ and $v$ field) for $P=3195$N, fringe interval 0.417$\mu$m. The numbers are fringe orders

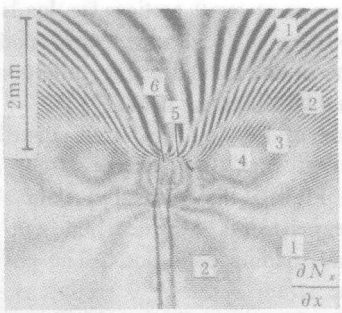


Fig .7 $\Delta N_x/\Delta x$ fringe pattern ($\varepsilon_x$ field) for $P=3195$N, $\Delta x=\Delta=0.213$mm, $1/f\Delta=0.00195$. The numbers are fringe orders

The second experiment was carried out in order to study crack initiation and crack growth. The span is increased to 48 mm. The specimen is loaded at three steps with loads 1065N 2130N and 3195N. When load $P$ is equal to 1065N, the crack has not initiated at the notch-tip, necking at the notch-tip has been started. For load $P=2130$ N the necking zone is extended, and a crack is initiated at the notch-tip. When load $P=3195$N the crack was extended to 0.62mm, and the number of fringes is increased rapidly. $N_x$ and $N_y$ fringe patterns at the crack-tip for load $P=3195$N is shown in Fig.6. The fringe density is very large, with an order of 42 line/mm. The necking zone is reduced significantly. Fig.7 gives $\Delta N_x/\Delta x$ fringe pattern of local zone at crack-tip.

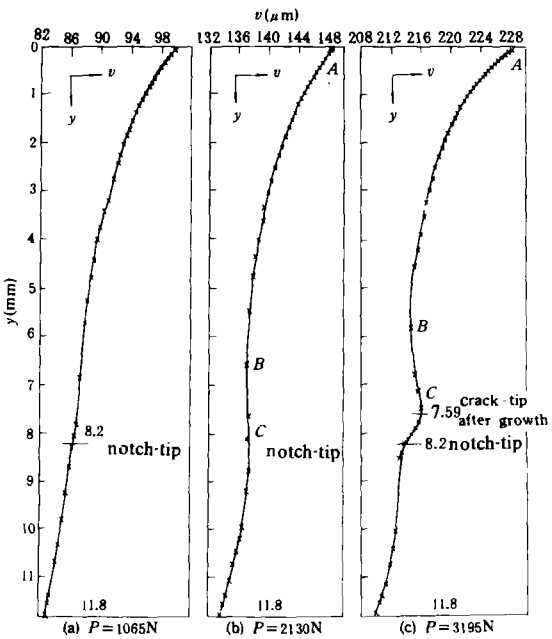


Fig.8 $v$-$y$ curve at $x=0$ section

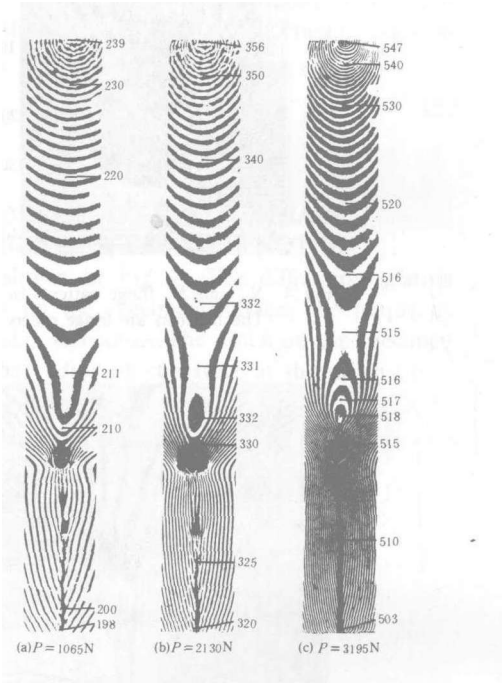


Fig.9 Ny fringe patterns $v$-displacement field, fringe interval 0.417 μm

Using $N_x$, $N_y$ fringe patterns and Eqns. (1) and (2), the displacement distribution curve at a section of specimen can be measured and calculated. The $y$ dircetion displacement distribution $v$-$y$ curves at $x=0$ section for loads 1065N, 2130N and 3195N are shown in Fig.8. The $N_y$ fringe pattern of local zone corresponding with Fig.8 is shown in Fig.9. The appearance of necking zone at the notch-tip, the initiation of crack at the notch-tip and the crack growth at the crack-tip can be observed from Fig.9.

In terms of Eq.(6) the strain distribution at a section can be obtained by displacement fringe patterns. Fig.10 gives the strain $\varepsilon_y$ distribution at $x=0$ section for loads 2130N and 3195N. In Fig.10 the measured data for load $P=2130$N by strain gage were also given. The two experiments were carried out on two specimens having identical geometric dimensions and loading conditions. The position of strain-gage on the specimen can be found from Fig.10. The strain $\varepsilon_y$ at $x=0$ section is changed from negative to positive, which can be observed in Fig.10. Accordingly, the slope of $v$-$y$ curve in Fig.8(b) and (c) is also changed from negative (AB) to positive (BC). The points B correspond to the null strain point in Fig.10. The data obtained by strain gage agree reasonable well with the results obtained by moire interferometry. They both depict the regularity of the strain $\varepsilon_y$ distribution at $x=0$ section.

The opening displacement at the notch-tip and the crack-tip are shown in Fig.11.

Fig.12 gives the strain $\varepsilon_x$ distribution at $x=0$ section obtained by Eq.(6). The $\varepsilon_x$ values at the notch-tip and the crack-tip for loads 1065N, 2130N and 3195N obtained from $\Delta N_x/\Delta x$ fringe patterns are 0.00501, 0.00688, and 0.01134, As compared with the results of Fig.12, the errors are 3.7%, 4.6% and 5.5%, respectively.

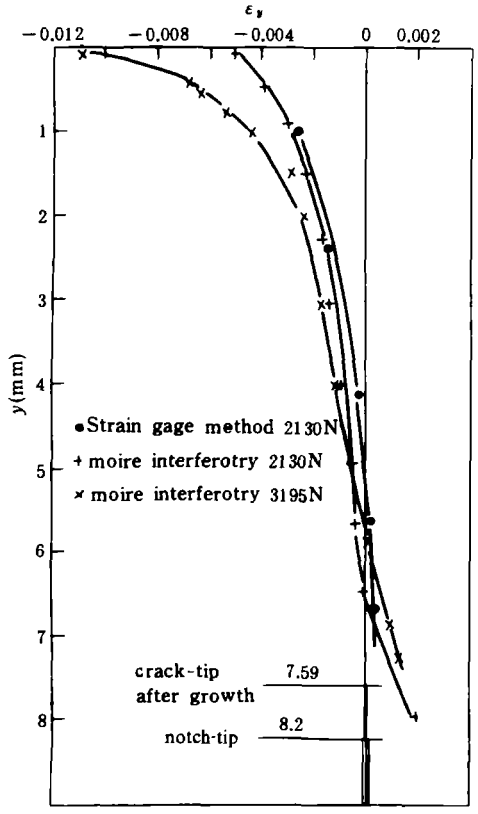


Fig.10 The strain $\varepsilon_y$ distribution at $x=0$ section

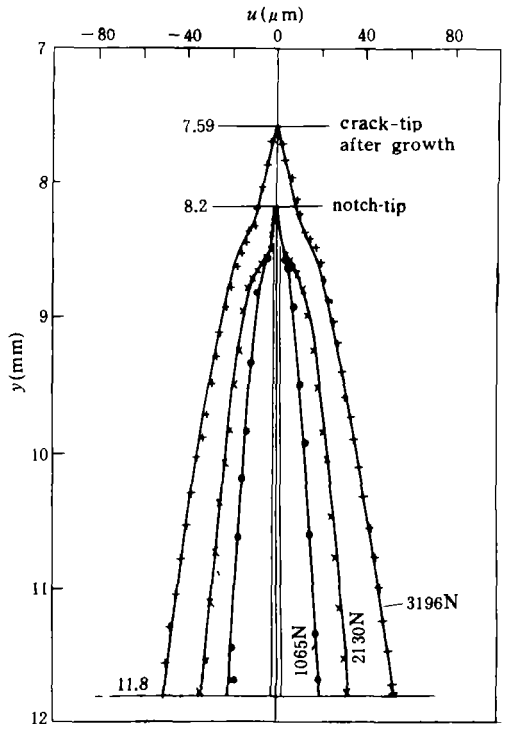


Fig.11 The opening displacement distribution at $x=0$ section

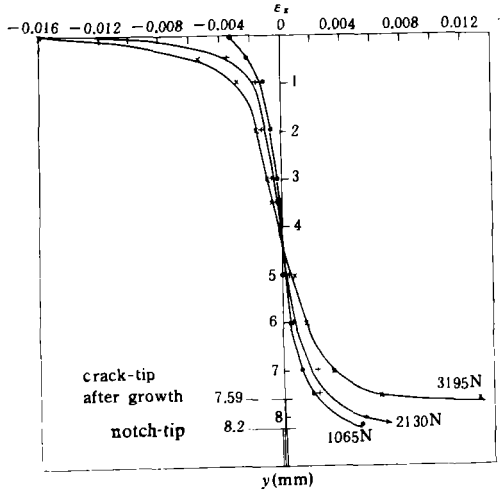


Fig.12 The strain $\varepsilon_x$ distribution at $x=0$ section

## IV. CONCLUSION AND DISCUSSION

1. A practical experimental arrangement for moire interferometry was given in this paper. The method of adjusting arrangement is explained by wave front interference theory.
2. The experiments of three point bending beam with crack using moire interferometry indicated that distribution for strain $\varepsilon_y$ at $x=0$ section along $y$ direction varies from negative to positive before and after crack growth.
3. the fringe distribution in the necking zone can be observed and the strain field at the notch-tip and the crack-tip can be measured. They can not be obtained by geometric moire or by speckle interferometry. For geometric moire, at necking zone the reference grating will be detached from specimen grating. For speckle interferometry, at necking zone, the interrelation of speckles will not hold. All of these show that the moire interferometry is superior.
4. The fringes of strain field obtained by moire interferometry are thick. If the carrier patterns and optical filtering technique are employed, then the interference of fringes of displacement field can be deleted but the speckle noise will appear. The fringes of strain are mixed up at stress centralized place, for example, at the crack tip[1]. However the fringes of displacement field possess subwavelength sensitivity, high spatial resolution and excellent fringe definition. The fringe densities exceeding 42 per mm have been realized in this paper. The strain precision obtained by Eq.(6) is much better. When the computer image processing equipment could be applied to moire interferometry, it would be more convenient and more accurate.
5. Due to the limit of grating area (maximum 70 mm × 70 mm) and of optical device bore, the moire interferometry can only be used to measure deformation of small area specimens, and the measurement must be carried out on an isolation table in a dark room.

**Acknowledgments**: The authors are grateful to Professer Dai Fulong of Tsinghua University for his helpful discussion.

## REFERENCES

[1] Post. D., et al. NASA Contractor Report No.3844 (1984).
[2] Dai Fulong, et al. *Optics and Laser in Engineering*, 12 (1990).